Characterization of the remaining material and mechanical properties of historic wooden foundation piles in Amsterdam

Pagella, Giorgio; Mirra, Michele; Ravenshorst, Geert; Gard, Wolfgang; van de Kuilen, Jan Willem

DOI
10.1016/j.conbuildmat.2024.138616

Publication date
2024

Document Version
Final published version

Published in
Construction and Building Materials

Construction and Building Materials 450 (2024) 138616

Contents lists available at ScienceDirect

Construction and Building Materials

journal homepage: www.elsevier.com/locate/conbuildmat

Characterization of the remaining material and mechanical properties of historic wooden foundation piles in Amsterdam

Giorgio Pagella [a,*,1], Michele Mirra [a,2], Geert Ravenshorst [a,3], Wolfgang Gard [a,4], Jan-Willem van de Kuilen [a,b,5]

[a] Delft University of Technology, Faculty of Civil Engineering and Geosciences, Biobased Structures and Materials, Delft 2628CN, the Netherlands
[b] Technical University of Munich, School of Engineering and Design, Wood Technology, München 80333, Germany

ARTICLE INFO

Keywords:
Wooden foundation piles
Micro-drilling
Bacterial decay
Mechanical properties
CT scanning
Strength Prediction

ABSTRACT

The majority of the bridges in the historic city centre of Amsterdam are supported by wooden foundation piles. Most of these were constructed 100–300 years ago, currently raising concerns about potential safety issues. The wooden piles under the bridges remain entirely under the water table, potentially subjected to bacterial decay in anaerobic conditions. Bacterial degradation proceeds at a slow rate, allowing the piles to perform their function for many years, although causing a reduction of their load-carrying capacity over time. To this end, a large experimental campaign was conducted to characterize the material and mechanical properties in relation to biological decay of 60 spruce and fir piles, dated back to 1727, 1886 and 1922, retrieved from two bridges in Amsterdam. Large-scale compression tests were carried out on 201 pile-segments extracted from head, middle-part and tip of the piles to determine their remaining short-term compressive strength. Micro-drilling measurements were conducted on each pile and analysed with a TU-Delft-developed algorithm, aimed at determining the *soft shell* – the width of the decayed outer layer of the piles' cross section. Micro-drilling allowed to accurately assess the remaining sound cross section of the pile, which resulted to be well correlated to its mechanical properties. The extent of decay throughout the cross-section of the piles was assessed within sapwood and heartwood through experimental models from literature and validated with Computed Tomography (CT) scanning. This allowed to identify that bacterial decay was only present in the non-durable sapwood, even in very degraded piles. Moreover, the soft shell resulted to be rather uniform along the piles' length. The analysis of decay, supported by micro-drilling and CT scans, allowed to develop experimental equations to predict the remaining short-term compressive strength along the pile length. The micro-drilling technique is now used on a large scale in Amsterdam, supporting the assessment of the remaining load carrying-capacity of wooden foundation piles in the city, aiding in the planning of conservation, maintenance and preservation strategies.

1. Introduction

1.1. Background

Many buildings and infrastructures in the city of Amsterdam (NL) are supported by wooden foundation piles. It is estimated that more than eleven million timber piles are present in the city [1]. Mostly pine, spruce, and alder piles were traditionally used, typically 10–12 m long and tapered, driven through the weak soil layers in order to reach the stable bearing sand layers (end bearing piles), with head diameter of 180–200 mm and tip diameter of 120–140 mm, as extensively reported in [1,2]. On top of the piles, the foundation system in Amsterdam was made by a horizontal cross- and longitudinal beams [3,4]. Timber pile foundations can be found in delta cities across European countries, such

* Corresponding author.
E-mail address: g.pagella@tudelft.nl (G. Pagella).
1 0000–0002-2552–4877
2 0000–0002-9898–8971
3 0000–0002-1462–5584
4 0000–0002-7734–4560
5 0000–0001-6974–3783

https://doi.org/10.1016/j.conbuildmat.2024.138616
Received 21 June 2024; Received in revised form 29 September 2024; Accepted 3 October 2024
Available online 5 October 2024

as Stockholm (SE), Hamburg (DE), and Venice (IT) [5-7], but also overseas locations including Boston (US) [1,2]. Even though the structural layout in the various locations may differ, the actual ageing processes are of similar nature [8]. The foundational system of timber piles can vary among cities, differing in construction technique, pile dimensions, lengths, and types of wood species used, depending on local environmental conditions, historical building practices, and the availability of materials [2]. Most of the timber foundations in Amsterdam were constructed 100–300 years ago, and the assessment of their state of conservation and remaining load-carrying capacity have become important [8–12]. When timber piles are in the ground below the water level, they can be subjected to biological decay which can strongly reduce their load-carrying capacity [13,5,6,14,15], leading to safety issues in the supported buildings [16–19,3,4,20,21]. Biological decay in waterlogged soils can be caused by either soft rot fungi (in low-oxygen conditions), or bacteria (even in anoxic conditions) [16,22-25]. More specifically, the latter are named erosion bacteria on the basis of their way of eroding the wood fibre cell walls [14,16], responsible for wood degradation in all types of waterlogged anaerobic terrestrial and marine environments worldwide. Bacterial decay proceeds more slowly over time than fungal attack, which cannot survive under water in absence of oxygen [16,17,20,26], but could cause a very fast degradation of timber piles, especially when the water level decreases exposing the piles to conditions where oxygen is present. Piles in anoxic conditions can perform their function for centuries before showing a substantial reduction of the load-carrying capacity [1]. Wooden foundation piles in The Netherlands, mostly comprise softwood species [17–19], susceptible to bacterial degradation in saturated soils, especially in Amsterdam where the piles remain submerged under the water level for all their service life. For submerged piles, bacterial attack always proceeds radially inward within their cross section, at first affecting the non-durable sapwood, while the inner part of the cross section, including the heartwood, tends to exhibit a lower degree of decay or remains sound [22,7,23,27,24,28–33]. However, decayed wooden piles can appear unaffected in the field, maintaining their shape and colour despite the degradation occurring [22,23]. This poses a challenge in the engineering assessment of historic wooden piles, exacerbated by the difficulty in inspecting the foundations hidden beneath the soil.

1.2. Scope of the research

Given the essential function of wooden pile foundations and their widespread presence in the historic city centre of Amsterdam, estimating their remaining material and mechanical properties in relation to biological decay is crucial for arranging timely maintenance interventions. As timber foundation piles were primarily designed on historical experience, the current material status can only be estimated through the assessment of the present structure.

To this end, the first scope of this research is to conduct an extensive experimental campaign, in collaboration with the municipality of Amsterdam [21], for assessing the impact of bacterial decay on the mechanical properties of wooden foundation piles and to explore assessment techniques for efficiently mapping the radial distribution of decay within these piles. More specifically, the physical and mechanical properties of 60 spruce (*Picea abies*) and fir (*Abies alba*) historic piles will be characterized, after they have been exposed in the soil for approximately 100, 135 and 295 years. The piles were retrieved from two bridges in Amsterdam that were demolished and replaced (See Chapter 2). The following techniques will be employed to achieve the fist objective of this research:

- Large-scale compression tests will be conducted on pile segments extracted from head, middle-part and tip of the piles, allowing to assess the remaining short-term compressive strength along the piles in relation to bacterial decay after three distinct periods of service time (Section 3.1).
- Micro-drilling measurements will be employed to determine the potential degraded portion of the cross section [4]. Micro drilling allows to inspect the material status throughout the whole cross section of the pile, involving the utilization of a drilling tool, where a drilling needle is pushed into the material with a chosen drill and feed speed, resulting in a graphical representation of the resistance encountered during the drilling process (Section 3.2). Among the available non-destructive techniques for assessing the state of conservation of wooden piles, micro-drilling stands out as a promising method [34–41]. With micro-drilling, an assessment of the material can be conducted in different positions and directions, independently from the pile's moisture content (as demonstrated in [40]), resulting in more available measurements, increased accuracy and faster in-situ testing. Based on the TU-Delft-developed algorithm for analysing micro-drilling signals of historic wooden piles, presented in [4], the decayed outer layer of the cross section of the piles can be accurately determined.
- The extent of decay from the wood surface inwards (measured with micro-drilling) will be compared to the proportion of sapwood and heartwood [42–46] (Section 3.3). The boundary between these two parts cannot be visually determined in the investigated historic spruce and fir piles, as their colour is uniform throughout their cross section [47]. Thus, experimental models from literature [48] will be employed, supported and validated by computed tomography (CT) scanning. This technology was already applied on part of the investigated piles (9 piles) in [49]. CT scans can provide a reliable picture of the proportion of sapwood and heartwood within the piles' cross section (Paragraph 3.3.1).

The second objective of this research is to predict the short-term remaining compressive strength of the historic piles based on micro-drilling measurements. From in-situ micro-drilling signals, a direct estimation of the remaining short-term compressive strength will be made. The information on the remaining short-term compressive strength and amount of decay among head, middle-part and tip of all piles will be used to investigate correlations among the parts. Based on the regression analysis of all the tested segments along each pile, a prediction equation for the short-term compressive strength of pile-tips will be proposed. This is especially relevant for in-situ assessment, where micro-drilling measurements can be conducted underwater only on the pile head, located below the water level and accessible. From the analysis of the pile head, a prediction of the tip can be made, which corresponds to the critical section of the tapered pile, since depending on soil conditions, the tip could be subjected to high stresses during service, primarily due to its smaller cross section. These experimental prediction equations can be adopted in practice for an estimation of the remaining compressive strength of the piles, keeping in mind that the mechanical properties of the historic wooden piles could vary depending on the load levels acting on the foundation piles for centuries.

2. Materials

The test material comprised 55 full-length spruce (*Picea abies*) and 5 fir (*Abies alba*) foundation piles, which were originally part of the foundation system of the piers of two bridges (called bridge 30 and 41) in the city of Amsterdam (Fig. 1). The piles were dated back to 1727 (30 piles), 1886 (16 piles), and 1922 (14 piles); the fir piles were all driven in 1886. All the piles were completely submerged under the water level. The piles were extracted in 2021 and stored in water tanks to preserve their saturated status. The dimensions and the tapering of the piles (per building year) are listed in Table 1. The dimensions of piles driven in 1922 and 1886 were comparable, while piles driven in 1727 were approximately 2 m shorter, with, on average, 40-mm smaller tip diameter (D_{tip}) and 30-mm smaller head diameter (D_{head}).

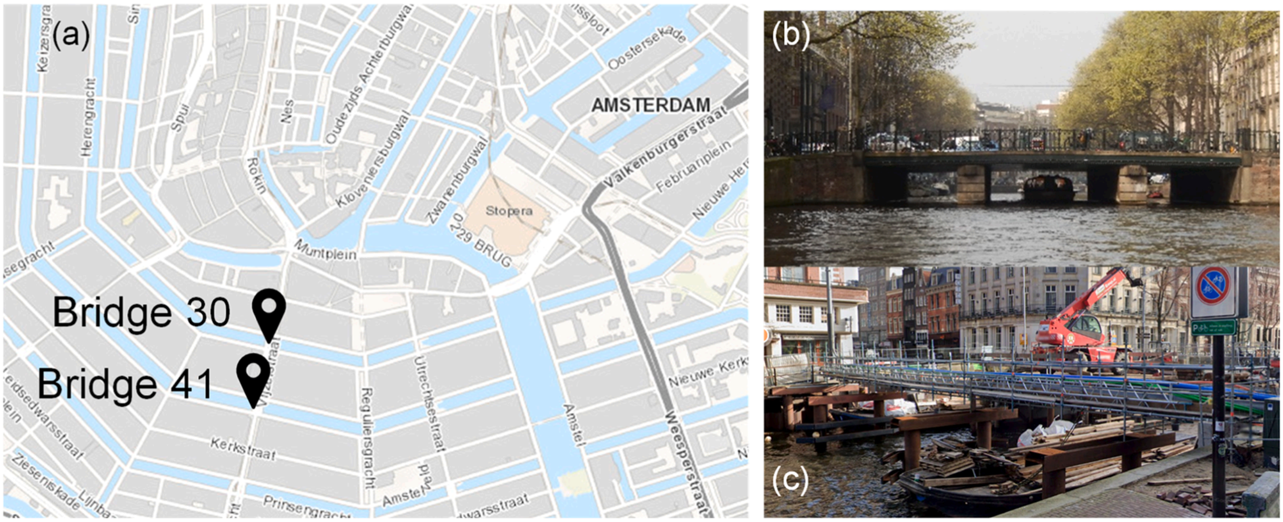

Fig. 1. (a) Locations in the historical city centre of Amsterdam from which the timber piles were extracted: (b) bridge 30 (De Isa van Eeghenbrug); (c) bridge 41 (Johanna Borskibrug).

Table 1
Data of full-scale piles retrieved from bridges in Amsterdam (Standard deviation reported in brackets).

Wood species	Building year	Bridge (No. of piles)	Length mean m	Diameter D_{head} mean mm	Diameter D_{tip} mean mm	Avg. tapering mm/m
Spruce	1922	B41 (14)	12.6 (0.8)	256 (12)	170 (16)	6.9 (1.5)
	1886	B30 (10); B41 (1)	12.0 (1.9)	248 (10)	172 (23)	6.4 (2)
	1727	B30 (15); B41 (15)	10.7 (1.1)	220 (39)	129 (29)	8.5 (2.9)
Fir	1886	B30 (3); B41 (2)	11.7 (1.9)	248 (13)	162 (32)	7 (2.5)

3. Methods

3.1. Compression tests parallel to the grain

The full-scale piles retrieved from bridge 30 and 41 were cut into head, middle and tip segments (Fig. 2) with a length of approximately 6 times the smallest diameter of the tapered log sections according to EN 408 [50]. This was done to investigate the compressive strength profile over the length of the tapered piles. During handling and cutting procedures, the piles were kept submerged in large water tanks to avoid drying and consequent cracking. Before testing, the pile segments remained completely submerged underwater for 20 days, with global moisture content (MC) for the whole cross section of all pile segments ranging from 60 % to 260 %, well above the fiber saturation point [51]. This was done to recreate the same in-soil conditions where the piles were fully under the water level, in order to obtain comparable mechanical and physical properties during testing. MC was determined with the oven-dry method, according to EN 13183 (2002) [52], for two 30-mm-thick discs taken from both sides of each selected segment. MC was calculated with input values of dry and wet mass of each pile segment; therefore, any variation of the wet mass of the pile could be related to a precise MC value. Compression tests were performed to determine the remaining short-term compressive strength ($f_{c,0,wet}$) and modulus of elasticity ($E_{c,0,wet}$) of the saturated pile segments in direction parallel to the grain. A displacement controlled set-up was used (Fig. 3), where the specimens were subjected to an axial load in direction parallel to the grain in accordance with EN 408 (2010) [50] and EN 14251 (2003) [53]. The displacement between the two steel plates during the mechanical testing was monitored using four linear potentiometers (S-sensors in Fig. 3), which were placed on the four edges of the top plate and connected to the bottom plate. The deformation of the specimens was measured with four linear potentiometers that were attached to the surface of the pile (P-sensors in Fig. 3), positioned at 90° intervals on each side of the pile, with a variable length equal to two-thirds of the length of the specimen. In addition, a hinge mounted on a steel plate was placed on top of the specimen to impart a uniformly distributed compression load on the pile. The tests were conducted at a displacement rate of 0.02 mm/s until the peak load was reached. After the peak load (reached at approximately 5 minutes according to EN 408 [50]), the test continued at a higher speed until the cracks were visible, and to show the post-peak behaviour of the pile [53]. Upon completion of the test, $f_{c,0,wet}$ was derived from the ratio between the maximum force reached in compression ($F_{c,0,test}$) and the average cross-sectional area of the each specimen. The $E_{c,0,wet}$ was calculated with the stress variation ($\Delta\sigma$) divided by the strain variation ($\Delta\varepsilon$), between 10 % and 40 % in the slope of the linear elastic portion of the stress-strain curve. In addition, the dynamic modulus of elasticity ($E_{c,0,dyn,wet}$) was determined through the frequency response method, using the timber grader MTG [54]. This measurement was performed on every segment prior to testing.

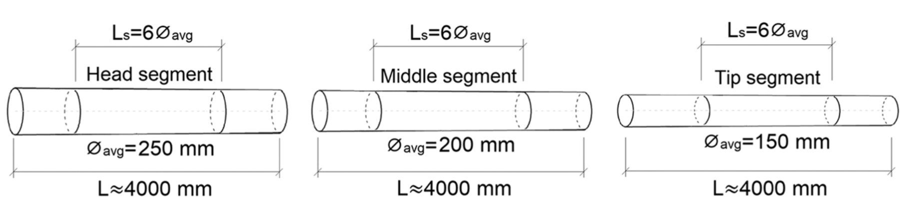

Fig. 2. Cutting scheme and subdivision of the full-scale pile into head, middle and tip segments.

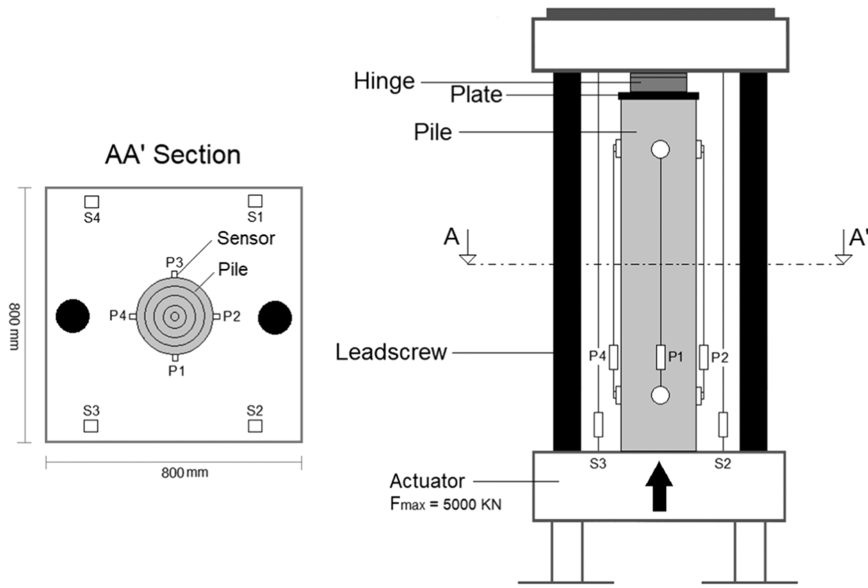

Fig. 3. Sensors positioning and set-up for the compression test of the pile segments.

3.1.1. Determination of the standardized density values

A reference density (ρ_{12}) at MC = 12 % was calculated for each pile segment with Eq. 1, from the calculated mass m_{12} (Eq. 2) and volume V_{12} at MC = 12 % (Eq. 3). This was done to have a standardized value for the density. In order to determine V_{12}, the volumetric shrinkage at MC = 12 % was calculated on the basis of the following three assumptions according to [51]: (a) shrinkage starts at the fiber saturation point (MC = 30 %); (b) the dimensions of the pile decrease linearly with decreasing MC; (c) variability in volumetric shrinkage can be expressed using a coefficient of variation of approximately 15 %, accounting for wood's intrinsic growth characteristics. Based on this, Eq. 3 was used to calculate the volume V_{12} at MC = 12 %.

$$\rho_{12} = m_{12} / V_{12} \tag{1}$$

$$m_{12} = m_{dry}\,(1 + u_{ref}) \tag{2}$$

$$V_{12} = V_{wet} \bullet (1 - S_0) \bullet (1 - u_{ref} / u_{30}) \tag{3}$$

Where: V_{wet} is the volume at test moisture content, u_{30} is the moisture content at fiber saturation point (assumed equal to 30 % [51]), u_{ref} is the moisture content at 12 %, S_0 is the volumetric shrinkage assumed to be equal to 12 % [51], from green (MC = 30 %) to ovendry (MC = 0 %) for both spruce and fir.

3.2. Micro-drilling measurements

Micro-drilling measurements were adopted in this research as assessment technique to investigate the potential degraded portion of the cross section of historic spruce and fir piles [34–41]. Micro-drilling was applied and calibrated for piles degraded by bacteria [4], after having conducted a more detailed characterization of the type of decay of 9/60 piles studied in this work from different construction years 1727 (3 piles), 1886 (4 piles), 1922 (2 piles) in [49]. The results from small-scale compression tests on wood samples extracted along the piles' cross section, Computed Tomography (CT) scans of the piles' cross section, and light microscopy observations on thin radial sections retrieved from the cross section in correspondence to the micro-drilling measurements (extensively reported in [49]), revealed that the investigated piles were decayed by bacteria. It was demonstrated that micro-drilling measurements are an effective method to analyse wood cross sections over a range of densities, either in case of sound or decayed wood, and resulted to be well correlated with the material properties of the piles, providing both qualitative and quantitative information on the degradation state of the pile. However, the bacterial degradation in wooden piles is still not well understood [55,27,34], and it should be noticed that it cannot be excluded a priori that other degrading agents, such as soft rot fungi (in low-oxygen conditions), might be present in isolated spot of the piles or in other timber piles in Amsterdam. In this context, an IML-RESI PD 400 tool [56] was used on the extracted historic wooden foundation piles (Fig. 4a). During micro-drilling measurements, a drilling needle is pushed into the cross-section with a drill speed of 2500 r/min and a feed speed of 150 cm/min. The needle used for the measurements is 400 mm long, with a thin shaft of 1.5 mm in diameter and a 3.1 mm wide triangular shaped cutting part, with hard chrome coating. The acquired data, recorded every 0.1 mm of the drilling depth, are plotted as resistance vs distance. Two micro-drilling measurements (A and B) were performed through the cross-section of each head-, middle- and tip-segment, approximately 90 degrees to each other and 300 mm from the head of the segment (Fig. 4b). In this way, it was possible to map the degradation pattern around the cross section and along the whole length of the pile, to study the possible amount of decay among head, middle-part and tip. Each measurement was performed on fully saturated pile segments, where high moisture contents revealed to have no influence on the decay levels detected with micro-drilling signals [40]. All segments were micro-drilled before mechanical testing, to have an accurate correlation between the material and mechanical properties. By observing the resistance profile of each micro-drilling signal, it is possible to distinguish wood annual rings: maximum amplitudes correspond to latewood rings; minimum amplitudes represent early-wood [42] (Fig. 4c). Isolated high or lower signal portions could also be detected in the micro-drilling signal, often associated to: wood knots [57,58] and other high density anatomical variations of the material (i.e. compression wood) [59–61], resulting in higher drilling amplitudes; piths and cracks in the cross-section, creating voids through which the drilling tool records zero or very low amplitude.

3.2.1. Determination of decay with micro-drilling

In order to evaluate the degraded portion of the cross section of the historic piles, the micro-drilling signals A and B performed on each pile segment were analysed with an algorithm developed by the TU Delft and presented in [4]. The purpose of the algorithm is to analyse the micro-drilling signal and to subdivide it in zones based on the signal amplitude. The algorithm is based on the differences in signal values and

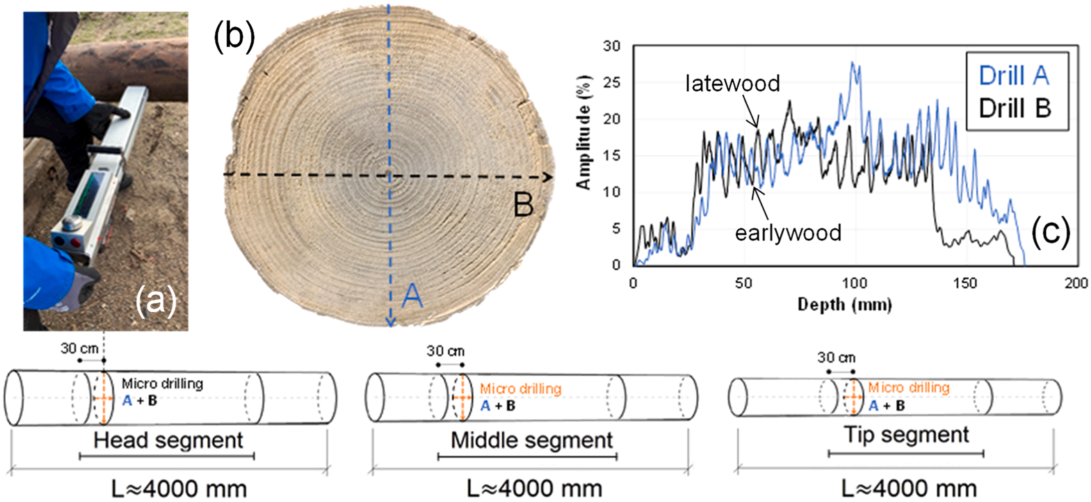

Fig. 4. (a) Micro-drilling measurements on a wooden pile; (b) drill A and B performed 30 cm from the head of the pile segment; (c) micro-drilling signal plotted as resistance (%) vs distance (mm).

not on absolute values, starting from the assumption that the wood in the centre of the pile is sound. First, the signal is smoothened to a Moving Average (Drill_MA) calculated between 5 mm before and 5 mm after a specific signal point. Then, an Incremental Outwards Moving Average (IOMA) is calculated on both sides from the centre of the pile. Thereby, the average of the Moving Average values is calculated starting from the centre, for both sides of the signal. The maximum IOMA value on both sides is considered to be the reference for sound wood. From this, four zones are determined through chosen ratios between the regular Moving Average of the signal and this maximum value of the IOMA. Zones 1, 2, 3, 4 on each side are determined as 20 %, 40 %, 60 %, 80 % of the moving average value with respect to the maximum value of the IOMA on that side, considered as reference for sound wood (Fig. 5a). The *soft shell* – the degraded portion of the cross section – is finally calculated as the sum of zones 1 and 2 (Fig. 5b), according to the calibration demonstrated in [4]. In this way, for each micro-drilling measurement, it is possible to assess the zone allocation in a relative way. It should be noticed that micro-drilling is a local measurement, thus it may happen that the soft shell measured in a cross section may differ if measured in other positions over the length of the specimen. In order to minimize this effect, all the micro-drilling measurements were performed in positions without visible defects or irregularities of the material. The total soft shell of a decayed cross section was calculated as the average of the 4 lengths of the soft shell (*SS*), corresponding to zones 1+2 on the left and right sides of micro-drilling signals A + B. From this, the average length of the soft shell (al_{SS}) was calculated with Eq. 4. This resulted in the assumption of a uniform distribution of decay around the cross section of the pile (Fig. 6). Subsequently, the remaining sound cross sectional area (A_{sound}), i.e. the part of the cross section that did not exhibit degradation, was calculated in Eq. 5, by subtracting al_{SS} (Eq. 4) to the radius (r) of the whole cross-section, and expressed as percentage of the full cross-sectional area (A_{tot}).

$$al_{SS} = (SS_{A,left} + SS_{A,right} + SS_{B,left} + SS_{B,right})/4 \tag{4}$$

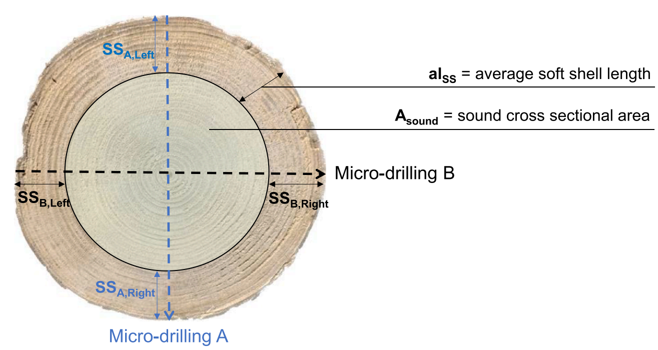

Fig. 6. Average soft shell length (al_{SS}) and remaining sound cross-sectional area (A_{sound}) calculated with soft shell left and right of micro-drilling signals A and B [4].

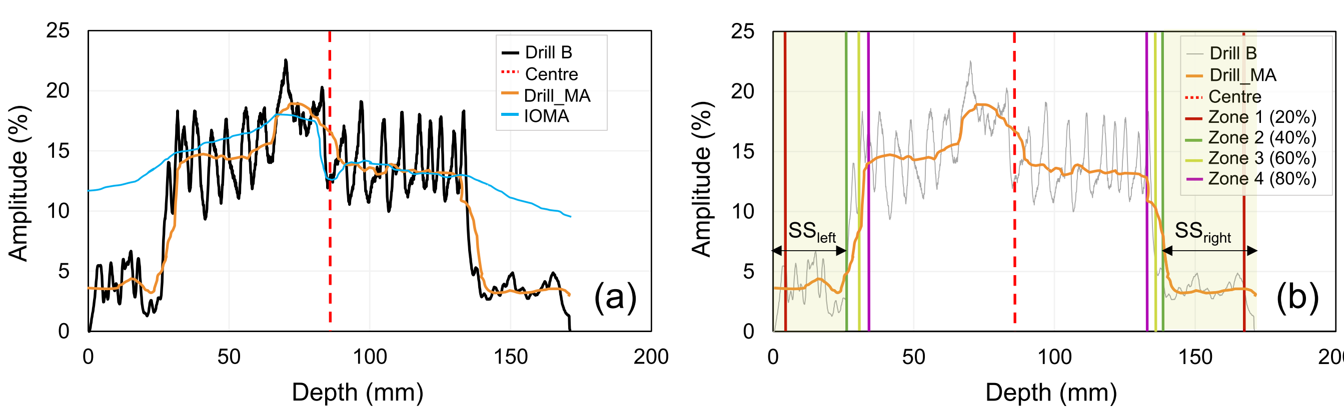

Fig. 5. Example of a drilling signal (Drill) of a decayed spruce pile: a) drilling moving average (Drill_MA) and IOMA from which the zones are calculated; (b) 4 zones and soft shell (SS_{left} and SS_{right}) associated to zone 1+2 according to [4].

$$A_{sound}\ (\%) = (A_{sound}\ /A_{tot})\cdot 100 = [\pi\ (r - al_{SS})^2\ /\ \pi r^2]\cdot 100 \quad (5)$$

3.2.2. Estimation of the equivalent sound compressive strength and stiffness

For all the 201 tested pile segments from 1922, 1886 and 1727, an equivalent sound compressive strength (EQ $f_{c,0,wet,sound}$) was derived in Eq. 6, calculated from the maximum force reached in compression ($F_{c,0,test}$) and A_{sound}. The equivalent stiffness (EQ $E_{c,0,wet}$) was also calculated in Eq. 7. Hereby the assumption is made that the soft shell will not take up forces, and zero strength and stiffness are allocated to this part, meaning that the entire force is taken up by the remaining sound cross-sectional area.

$$\text{EQ } f_{c,0,wet,sound} = F_{c,0,test}\ /\ A_{sound} \quad (6)$$

$$\text{EQ } E_{c,0,wet,sound} = (F_{c,0,test}\ /\ A_{sound})\ /\ (\Delta l\ /\ L_0) \quad (7)$$

Where: $\Delta l/L_0$ is the compressive strain.

3.3. Physical properties

The distribution of sapwood and heartwood within decayed piles, allows to understand the extent of bacterial decay within the cross section and whether decay is only limited to sapwood or whether it is present also in the heartwood. In the case of spruce and fir piles, sapwood and heartwood cannot be visually measured [62–64], since their colour is uniform throughout the cross section. Therefore, existing models from literature were employed [48], allowing to estimate the sapwood width (W_s) on the basis of diameter d (mm), number of annual rings (AR) and average radial growth rate RoG (mm/year) of a segment (Eq. 8).

$$W_s\ (\text{cm}) = (3.48\cdot \text{RoG}^{1.07})/(1+6.82\cdot e^{-0.064\ AR}) \quad (8)$$

The diameter, annual rings (AR) and rate of growth (RoG) of all the pile segments were measured. AR was calculated over the full radius R, by counting the annual rings [65]. RoG was calculated by counting the number of growth rings over the outer 75 % of the representative radius of the cross section in accordance with NEN-EN 1309–3 (2018) [65]. In case of extensive bacterial decay it was difficult to count all the rings, especially in the outer side of the cross section where the distinction between annual rings is less visible; therefore, a measurement error of 5–10 % should be considered.

The applicability of Eq. 8 from [48] was validated against the results from 49 saturated discs (150-mm thick) selected from the tested segments and subjected to CT scans (See Section 3.3.1). Only a limited number of discs were selected for undergoing CT scanning since it was not possible to perform CT scans on all piles' discs. CT scans on spruce and fir discs in wet (green) conditions can highlight the sapwood because of its larger moisture content and permeability compared to heartwood [62].

The proportion of juvenile wood was estimated in each pile segment, by measuring the length of the first 15 annual rings around the pith, corresponding to the juvenile wood [66]. Juvenile wood has a lower density compared to mature wood in softwoods such as spruce and fir, and often exhibits poorer mechanical properties [67,68]. The cross-sectional distribution of juvenile wood varies along the pile, being larger in the tip and decreasing towards the head (Fig. 7). This is a critical consideration, particularly regarding the pile tips examined in this paper, spanning from 25 to 50 years old, potentially containing a significant portion of juvenile wood within the heartwood. Should extensive decay occur in the sapwood, the strength of the pile may only rely on the remaining juvenile wood, which typically exhibits poorer mechanical properties. The physical properties of all the pile segments (percentage of sapwood, heartwood and juvenile wood of the total cross sectional area, diameter, AR and RoG) were characterized in order to find their correlations with the saturated short-term compressive strength of the piles.

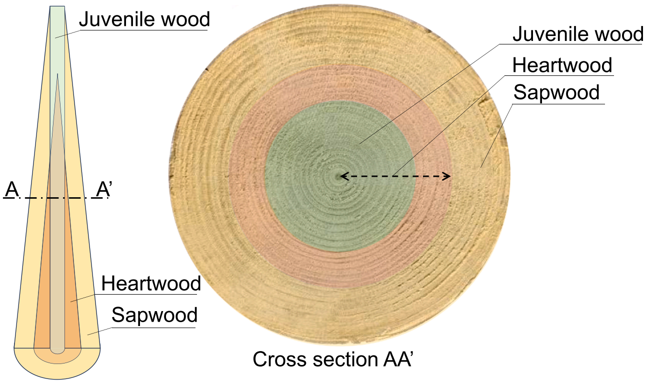

Fig. 7. Distribution of heartwood, sapwood and juvenile wood longitudinally along the pile and radially within the cross section of a spruce pile.

3.3.1. Validation of sapwood-heartwood proportion with CT scanning

CT scanning can provide a reliable picture of the proportion between sapwood and heartwood in saturated spruce and fir segments [62,69,70]. This is due to two main properties of sapwood in fully saturated conditions: a higher wet density compared to heartwood, due to the larger moisture content in saturated segments [42–46]. A *Siemens Somatom Definition* CT scanner was used, with a 0.6 mm sampling resolution. In this way, images from the segments were retrieved from X-rays by measuring the reflected radiations. The obtained images are displayed in grey values reported in Hounsfield units (HU) [71], with water having a value of 0 HU, tissues denser than water having positive values, and tissues less dense than water having negative values [71], up to −1000 HU for air. When using grey values, low-density tissues appear as darker (blacker) and high-density structures as brighter (whiter) colours. This results in a recognizable difference in grey values between sapwood (brighter colour = higher wet density) and heartwood (darker colour = lower wet density), as in Fig. 8 [72–74]. The sapwood width from CT scans was measured as average of four orthogonal measurements as shown in Fig. 8, and compared with the sapwood width (W_s) determined with Eq. 8 (Section 3.3). A total of 49 discs (150-mm thick) were CT scanned.

4. Test results

4.1. Mechanical properties of the historic piles

The results of large-scale mechanical testing are presented in Table 2, including a total of 201 pile segments extracted from 60 full-length spruce and fir piles, subdivided in head, middle-part and tip. No significant difference in the mechanical properties was found between building year 1922 and 1886, and between head and middle-part of spruce and fir piles from 1922, 1886 and 1727. The distribution of the

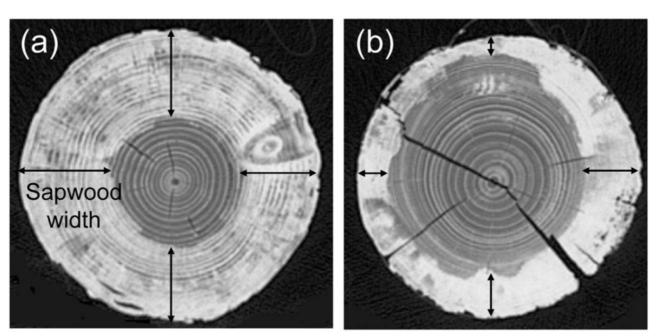

Fig. 8. Example of identification of sapwood (brighter) and heartwood (darker) in CT-scanned spruce (a) and fir (b) discs.

Table 2
Results for spruce and fir pile segments tested in compression parallel to the fiber in water saturated state according to EN 408. Mean values and standard deviation (SD) are reported.

Wood species	Building year	Part (No. segments)	$f_{c,0,wet}$ (MPa)		$E_{c,0,wet}$ (MPa)		ρ_{12} (kg/m^3)		D (mm)		MC (%)	
			mean	SD	mean	SD	mean	SD	mean	SD	mean	SD
Spruce (*Picea abies*)	1922/1886	Head/Middle (59)	13.8	2.1	9900	1580	470	43	240	18	80	21
		Tip (32)	11.8	2.1	8400	1610	450	48	190	15	95	24
	1727	Head/Middle (60)	7.5	2.4	5500	1890	380	52	200	34	160	48
		Tip (30)	5.8	1.8	4200	1590	360	47	150	27	195	54
Fir (*Abies alba*)	1886	Head/Middle (13)	15.1	2.1	11100	1770	490	41	220	30	100	24
		Tip (7)	12.0	3.0	9500	2420	460	70	160	29	100	19
"new piles" from [75], spruce (*Picea abies*)	"new"	Head/Middle (81)	16.9	2.4	10500	1600	490	40	240	20	85	15
		Tip (51)	14.4	2.1	8800	1750	470	55	180	17	90	16
"new piles" from [76], spruce (*Picea abies*)	"new"	No distinction (57)	20.0	2.2	-	-	-	-	140	12	110	28

data of $f_{c,0,\mathrm{wet}}$ and $E_{c,0,\mathrm{wet}}$ is shown in Fig. 9. The results showed that the short-term compressive strength of wooden piles that have been in service for a long time is lower than the strength values provided for 'new' saturated spruce characterized in Pagella et al. [75] and van de Kuilen [76] (Included in Table 2). This is partly due to the presence of decay (assessed in detail in [49]), especially for piles from 1727, with a service life of ca. 300 years (Paragraph 5.1). However, 2–5 MPa lower $f_{c,0,\mathrm{wet}}$ values were also determined for piles from 1922 and 1886 with a lower amount of decay (Paragraph 5.1).

4.2. Physical properties of the historic piles

The physical characterization of the piles presented in Table 3, showed no significant difference between the piles from 1922 and 1886. The spruce piles from 1727 had 10–15 annual rings less than 1922/1886, but resulted in similar RoG, due to average smaller diameters compared to piles from 1922/1886. The sapwood width (*Ws*) calculated according to Eq. 8 [48] (and validated in Section 4.2.1), allowed to determine the proportions of area (%) of sapwood, heartwood and juvenile wood, referred to the total cross-sectional area of the pile. An increasing % of heartwood area from tip to head was measured, and decreasing % of juvenile wood area to from tip to head. The average % area of juvenile wood in the tips reached approximately 85–95 % of the heartwood. The % of sapwood area slightly increased from head to tip, especially in spruce and fir piles from 1922/1886.

4.2.1. Validation of sapwood width with CT scanning

The CT scans conducted on the discs (according to Section 3.3.1) allowed to validate the sapwood width (*Ws*) estimated with the adopted model from literature [48]. As shown in Fig. 10, good correspondence between the actual and predicted sapwood width was obtained, independently of the construction year of the pile (1727, 1886, 1922) or of its wood species (spruce or fir). Therefore, the model in [48] was employed to estimate the sapwood width of all tested pile segments, in order to also investigate how deep bacterial decay has progressed within this portion of the cross section [49].

4.3. Relationships among the mechanical properties

The remaining short-term compressive strength for all the category of tested piles was correlated to the density adjusted to MC = 12 % (ρ_{12}). Both $f_{c,0,wet}$ and ρ_{12} (Fig. 11a), and $E_{c,0,wet}$ and ρ_{12} (Fig. 11b), were strongly correlated. In spruce piles from 1727, ρ_{12} was significantly lower compared to 1922/1886, possibly due to bacterial decay (Paragraph 5.1). The strong correlation between $f_{c,0,wet}$ and $E_{c,0,wet}$ (Fig. 12a), indicates that the stiffness is a good indicator for the wet compressive strength. A very similar correlation was also found between $f_{c,0,wet}$ and $E_{c,0,wet,dyn}$ (Fig. 12b), determined through frequency response measurements. This suggests that frequency response measurements can be used to efficiently estimate the modulus of elasticity of historic timber piles.

5. Analysis of the remaining short-term compressive strength in relation to bacterial decay

5.1. Assessment of decay with micro-drilling

The average soft shell length (al_{SS}) and the remaining sound cross-sectional area (A_{sound}) related to the remaining short-term compressive strength are presented for all historic pile segments in Table 4, based on the micro-drilling approach (Paragraph 3.2). Moreover, Table 4 lists the sapwood width (W_s) of the pile segments and the decayed percentage of sapwood depending on al_{SS}.

According to the small-scale characterization conducted in [49], the degradation was attributed to bacterial decay, confirming that the piles extracted from bridge 30 and 41 in Amsterdam remained submerged in anoxic conditions throughout their service life. However, it should be

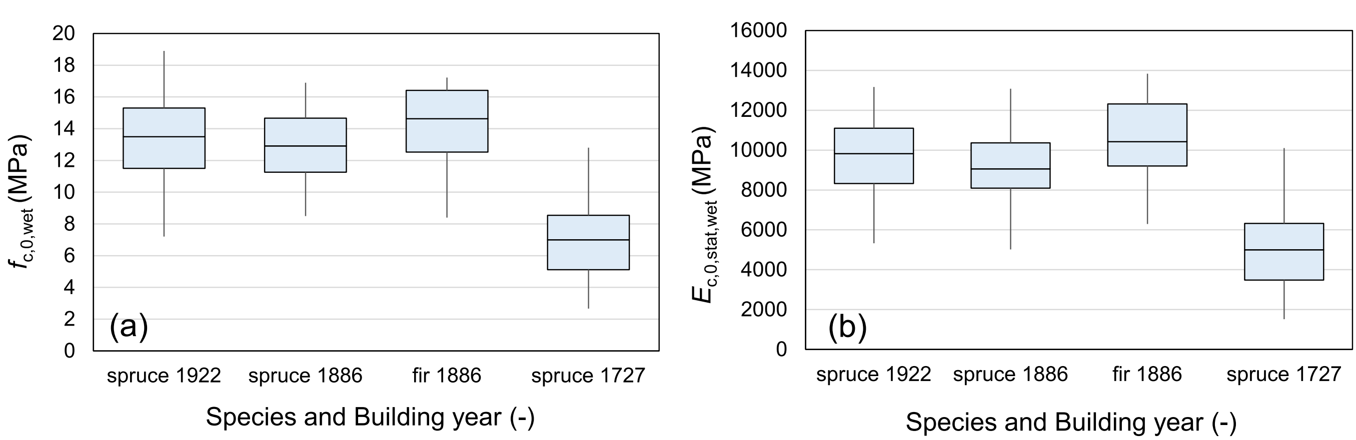

Fig. 9. Data distribution for (a) $f_{c,0,wet}$ and (b) $E_{c,0,wet}$ of spruce and fir pile segments divided in 3 building years (1922, 1886, 1727).

Table 3
Physical properties of head, middle-part and tip spruce and fir piles. The Area (%) of sapwood, heartwood and juvenile wood refers to the total cross-sectional area of the pile.

Wood species	Building year	Part (No. segments)	Diameter (mm)		AR (No. annual rings)		RoG (mm/year)		Sapwood Area (%)		Heartwood Area (%)		Juvenile wood Area (%)	
			mean	SD	mean	SD	mean	SD	mean	SD	mean	SD	mean	SD
Spruce	1922/ 1886	Head (29)	249	15	68	16	1.7	0.4	65	8	35	8	13	5
		Middle (30)	226	13	58	16	1.8	0.5	69	7	31	7	15	3
		Tip (32)	193	15	45	13	2.0	0.7	74	5	26	5	22	2
	1727	Head (30)	212	33	55	11	1.7	0.5	71	5	29	5	15	3
		Middle (30)	189	31	45	10	1.9	0.6	74	4	26	4	20	3
		Tip (30)	150	27	38	10	1.8	0.7	75	3	25	3	23	2
Fir	1886	Head (6)	235	30	72	19	1.5	0.4	63	9	37	9	12	3
		Middle (7)	208	25	57	16	1.6	0.4	69	7	31	7	16	5
		Tip (7)	162	29	46	11	1.5	0.3	72	4	28	4	22	5

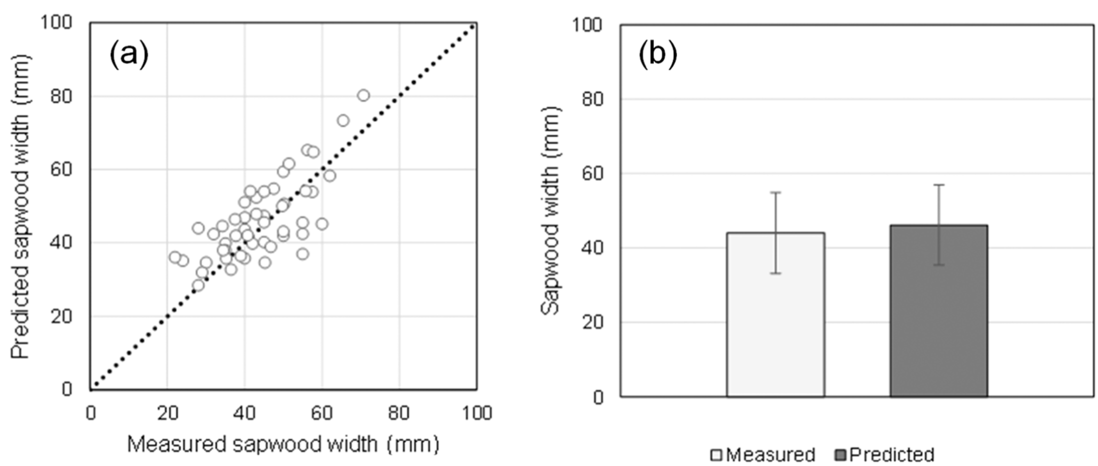

Fig. 10. Comparison between the sapwood width for 49 pile discs determined with CT scans and that predicted with the model of [48].

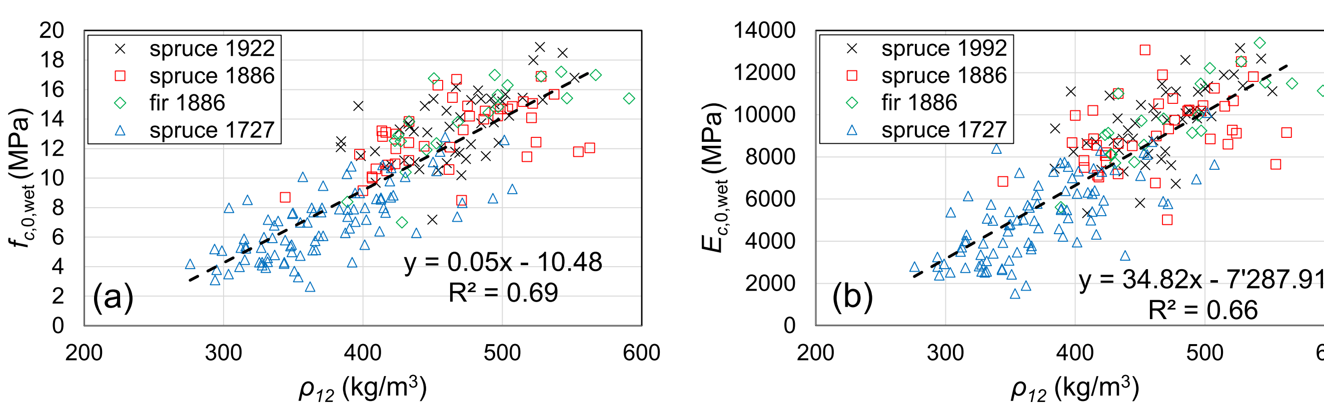

Fig. 11. Relationship between (a) $f_{c,0,wet}$ and density ρ_{12}; (b) $E_{c,0,wet}$ and density ρ_{12} for all the categories of tested pile segments.

noticed that it cannot be excluded a priori that other degradation types such as soft rot fungi (in low-oxygen conditions) might be present in isolated spot of the piles or in other timber piles in Amsterdam.

A larger amount of decay was determined for piles from 1727 compared to 1886/1922, where al_{SS} ranged at 20–22 mm, with no significant difference across head, middle and tip of the pile. This highlights that bacterial decay is potentially uniform along the pile length: a useful information for the in-situ assessment of historic wooden foundation piles. Although al_{SS} resulted to be constant along the piles, the pile geometry is tapered, meaning that the diameter decreases from head to tip, resulting in a lower average A_{sound} in the tips, compared to head and middle-part, for the same values of al_{SS} as shown in Fig. 13. This is showcased in Table 4, especially in tips from 1727, where A_{sound} values are 15–20 % lower compared to head/middle. The pile segments from 1922/1886 exhibited a smaller amount of decay, with al_{SS} below 7 mm, approximately constant along the pile. A_{sound} resulted to be on average uniform in head and middle-part from 1922/1886, with a slight decrease in the tips, due to their inherent smaller cross-sectional area. In fir piles, al_{SS} remained always below 2 mm indicating a very low amount of decay for this wood species, in line with [19,77]. However, due to the limited dataset of fir piles only from 1886, no relevant conclusions can be drawn.

For all piles, at cross-sectional level, bacterial decay was only present in the sapwood. The values of al_{SS} remained always below the sapwood width (*Ws*) in all pile segments (Table 4). No degradation was detected in the heartwood. This is in line with the research conducted in Mirra

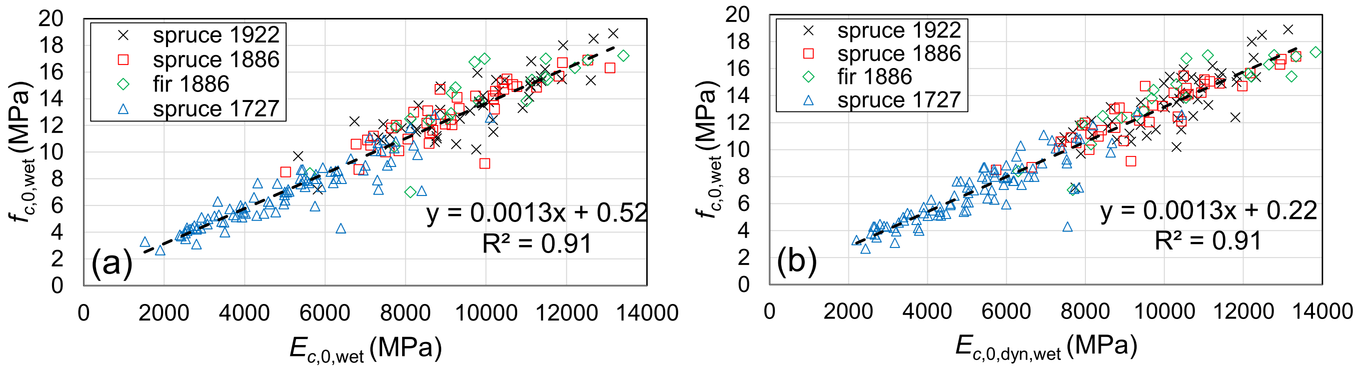

Fig. 12. Relationship between (a) $f_{c,0,wet}$ and $E_{c,0,wet}$; (b) $f_{c,0,wet}$ and $E_{c,0,dyn,wet}$ for all the categories of tested pile segments.

Table 4
Remaining short-term strength properties in relation to ρ_{12}, A_{sound}, al_{SS}, W_S and percentage of decayed sapwood.

Wood species	Building year	Part (No. segments)	$f_{c,0,wet}$ (MPa)		EQ $f_{c,0,wet,sound}$ (MPa)		ρ_{12} (kg/m^3)		A_{sound} (%)		al_{SS} (mm)		Ws[a] (mm)		Decayed sapwood width (%)	
			mean	SD	mean	SD	mean	SD	mean	SD	mean	SD	mean	SD	mean	SD
Spruce	1922/ 1886	Head (29)	13.9	2.0	15.3	2.5	465	42	91	8	6	5	52	8	14	14
		Middle (30)	13.7	2.3	14.7	2.3	470	45	94	7	4	4	50	7	9	10
		Tip (32)	11.8	2.1	13.7	2.4	450	48	87	10	7	5	47	5	18	13
	1727	Head (30)	7.5	2.3	12.2	3.3	385	55	63	14	22	11	49	10	53	20
		Middle (30)	7.3	2.4	12.3	2.9	375	48	62	20	20	11	46	9	52	28
		Tip (30)	5.8	1.8	11.6	2.4	360	47	50	15	22	9	38	7	66	20
Fir	1886	Head (6)	15.2	2.0	16.0	1.8	495	34	97	4	2	2	47	11	5	6
		Middle (7)	14.8	2.3	15.2	1.7	485	48	97	6	1	3	46	8	4	9
		Tip (7)	12.0	3.0	12.5	2.8	460	70	96	7	2	3	38	6	5	10

[a] calculated according to experimental model in [48] (See Paragraph 3.3).

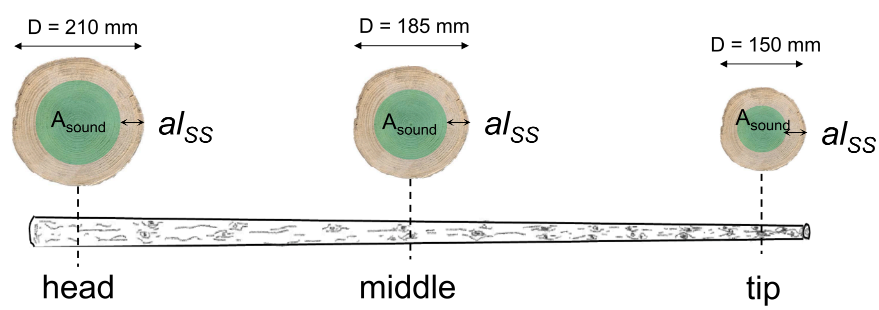

Fig. 13. Drawing of a decayed tapered pile with A_{sound} decreasing along its length for the same al_{SS} in head, middle-part and tip.

et al. [49] on selected timber piles tested in this work, where no signs of bacteria were found in the pile's heartwood, even in the most decayed piles from 1727. The same findings are also reported in literature [16,17,1], where the bacterial decay seemed to stop at the sapwood–heartwood boundary of spruce and pine, highlighting the very good durability of heartwood against bacterial decay. Yet, the inner heartwood of these piles did not show signs of decay and had properties in line with sound wood [1], once more proving the better resistance of heartwood against bacterial degradation, compared to sapwood. On average, the percentage of decayed sapwood width ranged at 50–63 % in spruce pile tips from 1727, with limited cases in which 90 % of the sapwood width resulted to be degraded. This suggests that the remaining sound cross section of these piles comprised a larger portion of sound heartwood, while most of the sapwood was decayed. A larger portion of heartwood would result in an intrinsic lower density (ρ_{12}), at similar RoG and Age. This is observable in Table 4, where ρ_{12} of piles from 1727 ranged at 360–385 kg/m^3, while ρ_{12} of piles from 1922/1886 ranged at 450–470 kg/m^3. This can also be explained by the lower EQ $f_{c,0,wet,sound}$ of piles from 1727, where A_{sound} comprised a larger portion of less dense heartwood and a smaller available sound sapwood portion due to extensive decay. The lowest values of ρ_{12} and EQ $f_{c,0,wet,sound}$ were determined for tips from 1727 in Table 4, attributable to the larger proportion of juvenile wood within their cross section, which closely aligned with the entirety of the heartwood (see Table 3). In piles from 1922/1886, the maximum percentage of average decayed sapwood remained within 20 % (Table 4), resulting in a larger contribution of sound available sapwood (above 80 %). In this case, only little variations in the density (ρ_{12}) and EQ $f_{c,0,wet,sound}$ were measured, especially in head and middle-parts. For tips from 1922/1886, approximately 10 % lower ρ_{12} and EQ $f_{c,0,wet,sound}$ values were determined compared to head/middle parts, possibly attributed to the larger portion of juvenile wood corresponding approximately to the whole heartwood (see Table 3).

5.2. Prediction of the short-term compressive strength in relation to bacterial decay

The remaining short-term compressive strength resulted to be well correlated with A_{sound} (Fig. 14), especially for the piles from 1727, which exhibited a larger range of A_{sound}, spanning from 25 % to 85 % of their full cross-sectional area. Fig. 14 showcases the presence of decay also in piles from 1922/1886, however limited to a lower range 65 % < A_{sound} < 100 % of the full cross-sectional area.

The remaining saturated short-term compressive strength of a pile can be estimated with Eq. 9, from the average reference $f_{c,0,wet,sound}$ = 14.74 MPa (Fig. 14), and A_{sound} (%) determined with micro-drilling. The experimental Eq. 9 is based only on A_{sound}, calculated through micro-drilling measurements and the diameter of the pile at the measurement location. This gives the possibility to have a direct estimation of the remaining short-term compressive strength from in-situ micro-drilling of the piles.

$$f_{c,0,wet} = 14.74 \quad e^{0.0182 \quad (A_{sound}-100)} \tag{9}$$

Based on the comparison of head and tip of all piles, an average decrease in $f_{c,0,wet}$ of 2 MPa in the tips compared to the pile heads was observed (Table 4). The relationship between $f_{c,0,wet}$ of head and tip of the pile can be used during the in-situ assessment of historic wooden foundation piles in Amsterdam to assess the remaining mechanical properties of the tip. The assessment of the remaining short-term compressive strength of the pile tip ($f_{c,0,wet,tip}$) is important, since the tip corresponds to the critical section of the pile, featuring the lowest compressive strength (Table 4). This could have an influence on the load-bearing capacity of the pile, where depending on soil conditions, the tip could be subjected to high stresses during service, primarily due to its smaller cross section.

Therefore, the pile head located below the water level can be accessed and inspected with underwater micro-drilling measurements [4] and its remaining short-term $f_{c,0,wet,head}$ can be predicted based on Eq. 9. Subsequently, based on the regression analysis of all the tested head and tip segments, Eq. 10 can be used in practice to estimate *Pred.* $f_{c,0,wet,tip}$ from $f_{c,0,wet,head}$. The correlation between *Pred.* $f_{c,0,wet,tip}$ and the actual $f_{c,0,wet,tip}$ determined with compression tests, is showcased in Fig. 15, showing a strong relationship between the two parameters and supporting the applicability of Eq. 10 in practice.

$$Pred. \quad f_{c,0,wet,tip} \quad = \quad 0.88 \quad f_{c,0,wet,head} - 0.76 \tag{10}$$

The presented approach for the direct prediction of the remaining short-term compressive strength on the basis of the micro-drilling signals is derived from the experimental analysis of the wooden piles presented in this paper. The experimental prediction equations can be adopted in practice for an estimation of the remaining compressive strength of the piles, keeping in mind that the mechanical properties of the historic wooden piles could vary depending on the load levels acting on the foundation piles for centuries. Further research is envisaged to investigate the remaining short-term compression tests of other wood species, in particular pine, very diffused in Amsterdam.

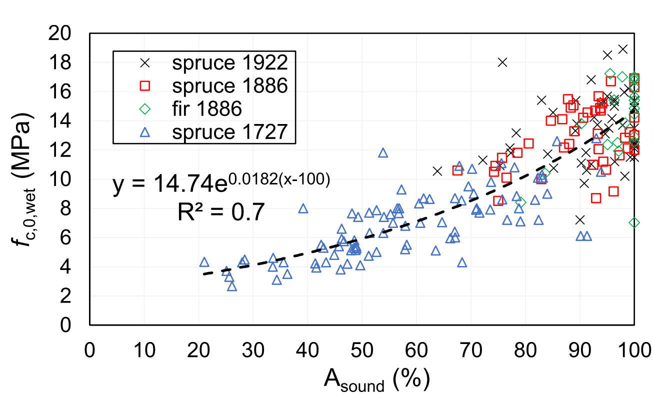

Fig. 14. Relationship between $f_{c,0,wet}$ and the percentage of sound cross-sectional area A_{sound} of all the historic spruce and fir segments.

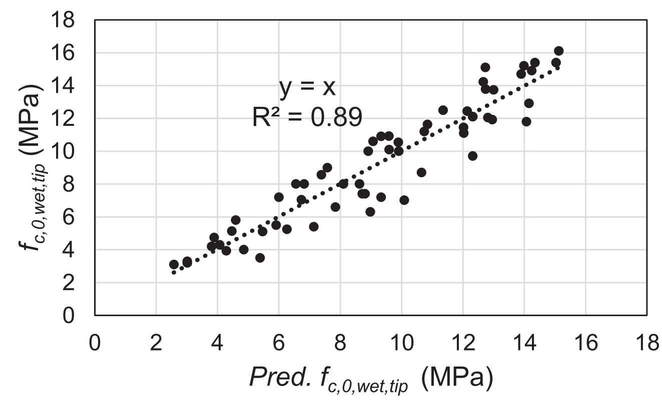

Fig. 15. Relationship between *Pred.* $f_{c,0,wet,tip}$ and $f_{c,0,wet,tip}$ based on the regression Eq. 10.

6. Conclusions

A total of 55 spruce (*Picea abies*) and 5 fir (*Abies alba*) historic piles that have been in service for 100, 135 and 295 years were retrieved from two bridges in Amsterdam and characterized in this research study. Their mechanical properties were determined by means of large-scale mechanical testing. The amount of bacterial decay along the piles could be reliably assessed with the innovative utilization of micro-drilling measurements. The extent of decay within the piles' cross section was analysed by estimating the portion of sapwood with empirical models from literature, which were successfully validated with computed tomography (CT) scanning of 49 discs extracted from the piles.

The results showed that the remaining short-term compression strength of wooden piles that have been in service for a long time is lower than the strength values provided for 'new' piles. This is partly due to the presence of decay, especially for piles from 1727, which were exposed to bacterial decay for 295 years. However, lower short-term compressive strength values were also determined for more recent piles from 1922 and 1886 (exposed to bacterial decay for ca. 100 and 135 years, respectively), which exhibited a lower amount of decay. These strength values have to be taken into account in future assessments of wooden foundation piles.

The micro-drilling approach allowed to estimate the *soft shell* of each pile: the degraded outer layer of the cross section to which zero remaining strength is assigned. The soft shell length (al_{SS}) was found to be rather uniform along the piles, from the head to the tip, with variations typically within ± 10 %. Bacterial decay was only present in the sapwood of the spruce and fir piles, also in very decayed piles from 1727. This is also supported by the findings in literature, where decay in spruce and fir piles never exceeded the sapwood–heartwood boundary.

The equivalent sound compressive strength assigned to A_{sound} of piles from all time periods could be determined, giving useful information about the remaining mechanical properties of the non-decayed part of the piles. The equivalent sound compressive strength of A_{sound} of piles from 1727 was lower than those from 1922 and 1886, due to a larger decayed portion of sapwood, resulting in a remaining A_{sound} with poorer mechanical properties, associated with the intrinsic lower compressive strength of heartwood and juvenile wood. However, this might also be partly attributed to the mechanical degradation due to higher stress levels during the service life of piles from 1727, associated with their larger presence of decay and thus a smaller sound load-bearing cross section.

As a result, micro-drilling can be effectively employed in-situ on the pile head to evaluate the remaining sound cross-section (A_{sound}), assuming uniform decay levels across the middle-part and tip of the piles. On the basis of the strong correlation between the remaining sound cross-sectional area (A_{sound}) and the short-term compressive strength of the piles, it was possible to predict their remaining short-term compressive strength. Experimental prediction equations were developed in this study, to be used in practice for estimating the remaining short-term compressive strength along the pile. From the underwater micro-drilling analysis of the pile head, the remaining short-term compressive strength of the tip can be experimentally derived. This constitutes an important step in the assessment of the remaining load carrying capacity of historic wooden piles, given that the tip corresponds to the critical section of the pile featuring the lowest mechanical properties, and depending on soil conditions, it could be subjected to high stresses during service due to its smaller cross section. It should also be noted that the mechanical properties of the piles could be different depending on the load levels acting on the foundation piles for centuries.

In conclusion, promising results were obtained in relation to the use of micro-drilling measurements for in-situ monitoring of historic wooden foundation piles, supported by the unique opportunity to characterize the material and mechanical properties of piles dated back to different construction years and with different decay levels. The micro-drilling technique is now used on a large scale in Amsterdam to retrieve signals that are useful for determining the soft shell, from which the remaining load carrying-capacity of wooden foundation piles can be estimated. The research conducted can aid the city of Amsterdam in arranging timely maintenance interventions, and contribute to the research framework supporting the development of deterministic models and reliability-based design assessment, including predictions for the remaining service life of timber pile foundations.

CRediT authorship contribution statement

Giorgio Pagella: Writing – review & editing, Writing – original draft, Visualization, Validation, Methodology, Investigation, Formal analysis, Data curation, Conceptualization. **Michele Mirra:** Writing – review & editing, Investigation. **Geert Ravenshorst:** Validation, Supervision, Project administration, Methodology, Funding acquisition. **Wolfgang Gard:** Project administration, Funding acquisition. **Jan-Willem van de Kuilen:** Validation, Supervision, Resources, Project administration, Funding acquisition.

Declaration of Competing Interest

The authors declare the following financial interests/personal relationships which may be considered as potential competing interests: Biobased structures and materials research group TU DELFT reports equipment, drugs, or supplies was provided by City of Amsterdam. If there are other authors, they declare that they have no known competing financial interests or personal relationships that could have appeared to influence the work reported in this paper.

Data Availability

The data that has been used is confidential.

Acknowledgments

The Authors gratefully acknowledge the Municipality of Amsterdam for having funded the research study and provided the analysed wooden foundation piles, as well as Ruben Kunz and Michael Lee, for their help in performing the experimental tests.

References

[1] Klaassen, R.K.W.M. et al. (2005). Preserving cultural heritage by preventing bacterial decay of wood in foundation poles and archaeological sites. Final report EVK4-CT-2001-00043. Wageningen 2005.
[2] R.K.W.M. Klaassen, J.G.M. Creemers, Wooden foundation piles and its underestimated relevance for cultural heritage, J. Cult. Herit. 13 (3) (2012) 123–128, https://doi.org/10.1016/j.culher.2012.02.014.
[3] W. Gard, G. Ravenshorst, J.W. van de Kuilen, Historical Wooden Pile Foundations in Amsterdam: An Integrated Approach for the Estimation of Structural Performance and Residual Service Life, in: Y. Endo, T. Hanazato (Eds.), SAHC 2023. RILEM Bookseries, vol 47, Springer, Cham, 2024.
[4] G. Pagella, G. Ravenshorst, M. Mirra, W. Gard, J.W. van de Kuilen, Innovative application of micro-drilling for the assessment of decay and remaining mechanical properties of historic wooden foundation piles in Amsterdam, ISSN 2666-1659, Dev. Built Environ. Volume 19 (2024) (2024) 100514, https://doi.org/10.1016/j.dibe.2024.100514.
[5] C. Bini, In Italian), in: G. Biscontin, F. Izzo, and, E. Rinaldi (Eds.), Il Sistema delle fondazioni lignee a Venezia - Valutazione del comportamento chimico-fisico e microbiologico, CORILA, Venice, 2009, pp. 9–24.
[6] J. Elam, C. Björdal, A review and case studies of factors affecting the stability of wooden foundation piles in urban environments exposed to construction work, ISSN 0964-8305, Int. Biodeterior. Biodegrad. Volume 148 (2020) (2020) 104913, https://doi.org/10.1016/j.ibiod.2020.104913.
[7] B. Pizzo, N. Macchioni, C. Capretti, E. Pecoraro, L. Sozzi, L. Fiorentino, Assessing the wood compressive strength in pile foundations in relation to diagnostic analysis: The example of the Church of Santa Maria Maggiore, Venice, ISSN 0950-0618, Constr. Build. Mater. Volume 114 (2016) 470–480, https://doi.org/10.1016/j.conbuildmat.2016.03.173.
[8] J.W.G. Van de Kuilen, Service life modelling of timber structures, Mat. Struct. 40 (2007) 151–161.
[9] Pagella, G., Ravenshorst, G.J.P., Wolfgang, G., van de Kuilen, J.W.G. (2022). Characterization and assessment of the mechanical properties of spruce foundation piles retrieved from bridges in Amsterdam. ICTB2021plus, Biel, Switzerland. https://doi.org/10.24451/cmes-1s31.
[10] Van de Kuilen, J.W.G., Beketova-Hummel, O., Pagella, G., Ravenshorst, G.J.P., Wolfgang G.: An integral approach for the assessment of timber pile foundations. In: World Conference on Timber Engineering 2021, WCTE 2021, pp. 2–8, Santiago, Chile (2021).
[11] M. Felicita, G. Pagella, G. Ravenshorst, M. Mirra, J.W. van de Kuilen, Assessment of in-situ stress distribution and mechanical properties of wooden foundation piles instrumented with distributed fiber optic sensors (DFOS) (Article), Case Stud. Constr. Mater. *20* (2024) e03139, https://doi.org/10.1016/j.cscm.2024.e03139.
[12] NEN 8707 (2018)+C2 (2023). Assessment of the structural safety of an existing structure during renovation and rejection - Geotechnical constructions, NEN.
[13] N. Macchioni, B. Pizzo, C. Capretti, Grading the decay of waterlogged archaeological wood according to anatomical characterisation, Int. Biodeterior. Biodegrad. 84 (2013) 54–64, 2013.
[14] A.P. Singh, Y.S. Kim, T. Singh, Bacterial degradation of wood, Second. Xylem Biol. (2016). Chapter 9, 2016.
[15] I. Irbe, O. Bikovens, V. Fridrihsone, M. Dzenis, Impact of biodeterioration on structure and composition of waterlogged foundation piles from Riga Cathedral (1211 CE), Latvia, J. Archaeol. Sci.: Rep. 23 (2019) 196.
[16] C.G. Björdal, J. Elam, Bacterial degradation of nine wooden foundation piles from Gothenburg historic city center and correlation to wood quality, environment and time in service, Int. Biodeterior. Biodegrad. 164 (2021).
[17] R.K.W.M. Klaassen, Bacterial decay in wooden foundation piles—Patterns and causes: A study of historical pile foundations in the Netherlands, ISSN 0964-8305, Int. Biodeterior. Biodegrad. Vol 61 (1) (2008) 45–60, https://doi.org/10.1016/j.ibiod.2007.07.006.
[18] U. Sass-Klaassen, T. Vernimmen, C. Baittinger, Dendrochronological dating and provenancing of timber used as foundation piles under historic buildings in The Netherlands, Int. Biodeterior. Biodegrad. 61 (1) (2008) 96–105.
[19] Klaassen, R.K.W.M. et al. (2005). Preserving cultural heritage by preventing bacterial decay of wood in foundation poles and archaeological sites. Final report EVK4-CT-2001-00043. Wageningen 2005.
[20] Varossieau, W.W. (1949). Opgegraven en aangetast hout vanuit biologisch oogpunt bezien. CIMO Delft, 1949 (in Dutch).
[21] Pagella, G., Ravenshorst, G.J.P., Wolfgang, G., van de Kuilen, J.W.G.: Characterization and assessment of the mechanical properties of spruce foundation piles retrieved from bridges in Amsterdam. International Conference on Timber Bridges ICTB2021plus, Biel, Switzerland (2022) https://doi.org/10.24451/cmes-1s31.
[22] C.G. Björdal, Microbial degradation of waterlogged archaeological wood, J. Cult. Herit. 13 (3) (2012) 118–122, 2012.
[23] A.P. Singh, Y.S. Kim, R.R. Chavan, Advances in Understanding Microbial Deterioration of Buried and Waterlogged Archaeological Woods: A Review, Forests 13 (2022) 394.
[24] I. Irbe, O. Bikovens, V. Fridrihsone, M. Dzenis, Impact of biodeterioration on structure and composition of waterlogged foundation piles from Riga Cathedral (1211 CE), Latvia, J. Archaeol. Sci.: Rep. 23 (2019) 196, 2019.
[25] Varossieau, W.W. (1949). Opgegraven en aangetast hout vanuit biologisch oogpunt bezien. CIMO Delft, 1949 (in Dutch).
[26] C. Wang, R.H. Leicester, M. Nguyen, Probabilistic procedure for design of untreated timber poles in-ground under attack of decay fungi, Reliab. Eng. Syst. Saf. 93 (2008) 476–481.
[27] A.P. Singh, Y.S. Kim, T. Singh, Bacterial degradation of wood, Second. Xylem Biol. (2016). Chapter 9, 2016.
[28] D.M. Holt, E.B. Jones, Bacterial degradation of lignified wood cell walls in anaerobic aquatic habitats, Appl. Environ. Microbiol. 46 (3) (1983) 722–727, 1983.
[29] G.F. Daniel, T. Nilsson, the, IRG/WP/1283, in: Ultrastructural Observations on Wood Degrading Erosion bacteria, 1986, International Research Group on Wood Preservation, 1986.

[30] Y.S. Kim, A.P. Singh, Micromorphological characteristics of wood biodegradation in wet environments: A review, IAWA J. 21 (2) (2000) 135–155, 2000.
[31] N.B. Pedersen, C.G. Björdal, P. Jensen, C. Felby, Bacterial Degradation of Archaeological Wood in Anoxic Waterlogged Environments. The royal chemical Society, Cambridge, RSC Publishing, 2013, p. 2013.
[32] A.P. Singh, A review of microbial decay types found in wooden objects of cultural heritage recovered from buried and waterlogged environments, J. Cult. Herit. 13S (2012) S16–S20, 2012.
[33] M. Mirra, G. Pagella, M. Lee, W. Gard, G. Ravenshorst, G.J.W. Van de Kuilen, Characterisation of bacterial decay effects on wooden foundation piles across various historical periods, ISSN 0950-0618, Constr. Build. Mater. Volume 421 (2024) (2024) 135670, https://doi.org/10.1016/j.conbuildmat.2024.135670.
[34] Gard W.F., Van de Kuilen, J.W.G. (2018) Micro-drilling resistance measurements of dense hardwoods for hydraulic structures. WCTE - World Conference on Timber Engineering, Seoul, South-Korea.
[35] E. Sharapov, X. Wang, E. Smirnova, J.P. Wacker, Wear behavior of drill bits in wood drilling resistance measurements, Wood Fiber Sci. 50 (2018) 154–166.
[36] S. Gao, X. Wang, B.K. Brashaw, R.J. Ross, L. Wang, Rapid Assessment of Wood Density of Standing Tree with Nondestructive Methods – A review. Proceedings of 2012 International Conference on Bio-based Material Science and Engineering, IEEE, 2012.
[37] L. Nutto, T. Biechele, Drilling resistance measurement and the effect of shaft friction – using feed force information for improving decay identification on hard tropical wood, : 19th Int. Nondestruct. Test. Eval. Wood Symp. (2015) 154–161.
[38] V. Gendvilas, G.M. Downes, M. Lausberg, J.J. Harrington, D.J. Lee, Predicting Wood Density Using Resistance Drilling: The Effect of Varying Feed Speed and RPM, Forests *15* (2024) 579, https://doi.org/10.3390/f15040579.
[39] M. Humar, A. Balzano, D. Kržišnik, B. Lesar, Assessment of wooden foundation piles after 125 years of service, Forests 12 (2021) 143, 2021.
[40] Mirra, M., Pagella, G., Gard, W.F., Ravenshorst, G.J.P., van de Kuilen, J.W.G. (2023). Influence of moisture content on the assessment of decay levels by micro-drilling measurements in wooden foundation piles. World Conference on Timber Engineering, Oslo, Norway, 2023.
[41] T.P. Nowak, J. Jasieńko, K. Hamrol-Bielecka, In situ assessment of structural timber using the resistance drilling method – Evaluation of usefulness, Constr. Build. Mater. 102 (2016) 403–415, 2016.
[42] Kollmann F., Côté, W.A. (1968). Principles of Wood Science and Technology. Springer-Verlag, Berlin · Heidelberg 1968, Ed. 1, 1968, 592 p, ISBN 978-3-642-87930-2. https://doi.org/10.1007/978-3-642-87928-9.
[43] M. Millers, The proportion of heartwood in conifer (Pinus sylvestris L., Picea abies [L.] H. Karst.) trunks and its influence on trunk wood moisture, J. For. Sci. 59 (8) (2013) 295–300, 2013.
[44] P. Gjerdrum, Heartwood in relation to age and growth rate in Pinus sylvestris L. in Scandinavia, Forestry 76 (2003) 413–424.
[45] B.J. Zobel, J.P. Van Buijtenen, Wood variation: its causes and control, Springer, Berlin, 1989, p. 363.
[46] S. Chauhan, R. Donnelly, Cl Huang, R. Nakada, Y. Yafang, J.C.F. Walker, Wood quality: in context. Primary Wood Processing, Springer, Dordrecht, 2006, https://doi.org/10.1007/1-4020-4393-7_5.
[47] Wagenführ, R. (2006) Holzatlas (Timber Atlas). Fachbuchverlag Leipzig, München.
[48] A. Sellin, Sapwood amount in Picea abies (L.) Karst. Determined by tree age and radial growth rate, Holzforschung 50 (1996) 291–296.
[49] M. Mirra, G. Pagella, M. Lee, W. Gard, G. Ravenshorst, G.J.W. Van de Kuilen, Characterisation of bacterial decay effects on wooden foundation piles across various historical periods, ISSN 0950-0618, Constr. Build. Mater. Volume 421 (2024) (2024) 135670, https://doi.org/10.1016/j.conbuildmat.2024.135670.
[50] EN 408 (2010) + A1 (2012): Timber structures–structural timber and glued laminated timber–determination of some physical and mechanical properties. European Committee for Standardization (CEN).
[51] Ross, R.J. (2021). Wood handbook wood as an engineering material. Forest Products Laboratory. General Technical Report FPL-GTR-282. Madison, WI: U.S. Department of Agriculture, Forest Service, Forest Products Laboratory. 543 p.
[52] NEN-EN 13183-1 (, NEN, 2002.
[53] . EN 14251 (2003) Structural round timber - Test methods. European Committee for Standardization (CEN).
[54] Ravenshorst, G.J.P., Van de Kuilen, J.W.G. (2009). Relationships between local, global and dynamic modulus of elasticity for soft- and hardwoods. CIB W18, proceedings paper 42-10-1, Dubendorf, Switzerland, 2009.
[55] T.P. Nowak, J. Jasieńko, K. Hamrol-Bielecka, In situ assessment of structural timber using the resistance drilling method – Evaluation of usefulness, Constr. Build. Mater. 102 (2016) 403–415.
[56] ⟨https://www.iml-service.com/product/iml-powerdrill/⟩. Last visited 19.3.2024.
[57] Pagella, G., Mirra, M., Ravenshorst, G.J.P., van de Kuilen, J.W.G.: Influence of knots and density distribution on compressive strength of wooden foundation piles. In: Current Perspectives and New Directions in Mechanics, Modelling and Design of Structural Systems, 1st edition CRC Press, London. Proceedings of The Eighth International Conference on Structural Engineering, Mechanics and Computation, Cape Town, South Africa, (2022) https://doi.org/10.1201/9781003348450-277.
[58] C.B. Caceres, L. Uliana, R.E. Henrandez, Orthogonal cutting study of wood and knots of white spruce, Wood Fiber Sci. vol. 50 (1) (2018) 55–65, https://doi.org.10.22382/wfs-2018-006.
[59] P. Hoffmeyer, Technical University of Denmark. Byg Rapport, role grain angle, knots, Tens. wood, Compress. wood, Other Anom. Mech. Prop. wood (1987). No. TR-183.
[60] S. Namari, L. Drosky, B. Pudlitz, P. Haller, A. Sotayo, D. Bradley, S. Mehra, C. O'Ceallaigh, A.M. Harte, I. El-Houjeyri, M. Oudjene, Z. Guan, Mechanical properties of compressed wood, ISSN 0950-0618, Constr. Build. Mater. Volume 301 (2021) (2021) 124269, https://doi.org/10.1016/j.conbuildmat.2021.124269.
[61] B. Gardiner, E. Macdonald, Compression wood in conifers – the characterisation of its formation and its relevance to timber quality, Eur. Union-Framew. Program. FP5-Qual. Life Manag. Living Resour. (2005) 376. QLRT-2000-00177,.
[62] F. Longuetaud, F. Mothe, J.-M. Lebsan, A. Makela, Picea abies sapwood width: variations within and between trees, Scand. J. For. Res. 21 (1) (2007) 41–53.
[63] M. Jakubowski, W. Koszewski, Proportion of sapwood and heartwood in stems of Norway spruce in mountain sites conditions, Ann. Wars. Univ. Life Sceinces. For. Wood Technol. 55 (2004) 259–262.
[64] M. Millers, The proportion of heartwood in conifer (Pinus sylvestris L., Picea abies [L.] H. Karst.) trunks and its influence on trunk wood moisture, J. For. Sci. 59 (8) (2013) 295–300.
[65] NEN-EN 1309-3 (2018): Round and sawn timber - Methods of measurements - Part 3: Features and biological degradations. NEN.
[66] B.J. Zobel, J.R. Sprague, Characteristics of Juvenile Wood. Juvenile Wood in Forest Trees. Springer Series in Wood Science, Springer, Berlin, Heidelberg, 1998, https://doi.org/10.1007/978-3-642-72126-7_2.
[67] J.H. Blohm, R. Evans, G. Koch, U. Schmitt, Identification and characterisation of Douglas-fir (Pseudotsuga menziesii (Mirb.) Franco) juvenile and adult wood grown in southern Germany, Drewno 59 (197) (2016) 41–47, https://doi.org/10.12841/wood.1644-3985.c01.05.
[68] V. Gryc, H. Vavrčík, K. Horn, Density of juvenile and mature wood of selected coniferous species, J. For. Sci. 57 (3) (2011) 123–130, https://doi.org/10.17221/18/2010-JFS.
[69] K. Sandberg, Nor. Spruce Heart – Prop. Relat. Outdoor Use Dr. Thesis, Lulea-.-. Univ. Technol. (2009).
[70] J.H. Fromm, I. Sautter, D. Matthies, J. Kremer, P. Schumacher, C. Ganter, Xylem water content and wood density in spruce and oak trees detected by high-resolution computed tomography, Plant Physiol. 127 (2) (2001) 416–425.
[71] C. Freyburger, F. Longuetaud, F. Mothe, T. Constant, J.-M. Leban, Measuring wood density by means of X-ray computer tomography, Ann. For. Sci. 66 (8) (2009) 804.
[72] W. Scheiding, M. Direske, M. Zauer, Water absorption of untreated and thermally modified sapwood and heartwood of Pinus sylvestris L, Eur. J. Wood Wood Prod. 74 (2016) 585–589.
[73] M. Fredriksson, O. Lindgren, End grain water absorption and redistribution in slow-grown and fast-grown Norway spruce (Picea abies (L.) Karst.) heartwood and sapwood, Wood Mater. Sci. Eng. 8 (4) (2013) 245–252.
[74] T. Sjökvist, M.E.P. Wålinder, Å. Blom, Liquid sorption characterisation of Norway spruce heartwood and sapwood using a multicycle Wilhelmy plate method, Int. Wood Prod. J. 9 (2) (2018) 58–65.
[75] Pagella, G., Ravenshorst, G.J.P., Gard, W.F., Van de Kuilen, J.W.G. (2024). Characterization of the mechanical properties of saturated spruce (*Picea abies*) and pine (*Pinus sylvestris*) foundation piles. Journal of Building Engineering. (Forthcoming).
[76] Van de Kuilen, J.W.G.: Bepaling van de karakteristieke druksterkte van houten heipalen. Toegepast-Natuurwetenschappelijk Onderzoek (TNO), order Nr. 94-con-RO271. Delft, The Netherlands. (1994) (in Dutch).
[77] R.K.W.M. Klaassen, B.S. van Overeem, Factors that influence the speed of bacterial wood degradation, J. Cult. Herit. 13S (2012) S129–S134, 2012.